

Photometric study of the over-contact binary star GSC 3822-1056^{★,★★}

Sz. Csizmadia¹, I. B. Bíró^{2,3}, and T. Borkovits²

¹ Konkoly Observatory of the Hungarian Academy of Sciences, PO Box 67, 1525 Budapest, Hungary

² Baja Astronomical Observatory of Bács-Kiskun County, PO Box 766, 6500 Baja, Szegedi út, Hungary
e-mail: borko@electra.bajaobs.hu; barna@electra.bajaobs.hu

³ Guest observer at the Instituto de Astrofísica de Canarias, Spain

Received 12 September 2002 / Accepted 7 March 2003

Abstract. Here we present the first Johnson-Cousins VR_C light curves of the over-contact binary star GSC 3822-1056. A period study and the light curve solution are also given. An extremely high rate of period increase (+11.6 s/century) was found. The origin of this period change can be: (i) partly covered light-time effect due to the orbital motion around the mass center of a possible third body; (ii) mass transfer between the components.

The light curve was solved using the 1998 Wilson-Devinney Code. We examined the light curve with and without third light. Both solutions yielded a contact configuration with high temperature difference between the components. Despite the high degree of the contact ($f = 0.57$), the temperature difference between the components $\Delta T = T_{\text{primary}} - T_{\text{secondary}} = 1045$ K. The high mass ratio of the system and its other unusual properties suggest that GSC 3822-1056 may be a recently formed contact binary.

Key words. techniques: photometric – stars: binaries: eclipsing – stars: binaries: close – stars: individual: GSC 3822-1056

1. Introduction

GSC 3822-1056 was independently found to be variable by Martin (2000) and Bíró (2000a) during the observations of the novalike variable DW UMa¹. Martin (2000) regarded it to be a δ Scuti variable, estimated from single band photometry. According to the colour indices of the system (see the next section), the spectral type can be estimated to be mid-G, which is inconsistent with a δ Scuti type classification, since δ Scutis commonly are of A0–F5 spectral type. Also the light curve (see Figs. 2 and 3) shows alternate minima with different depths repeating cyclically. Therefore Bíró (2000a) concluded that this object is a β Lyr-type eclipsing binary star.

Up to now, no light-curve solution has been published; therefore we decided to study GSC 3822-1056 photometrically.

Send offprint requests to: Sz. Csizmadia,
e-mail: csizmadia@konkoly.hu

* Observations were made by the 80 cm “IAC80” telescope at Observatorio del Teide in Tenerife, Spain, operated by Instituto de Astrofísica de Canarias.

** Tables 2a–c are only available in electronic form at the CDS via anonymous ftp to cdsarc.u-strasbg.fr (130.79.128.5) or via <http://cdsweb.u-strasbg.fr/cgi-bin/qcat?J/A+A/403/637>

¹ The coordinates given for GSC 3822-1056 in Martin’s paper and repeated in Bíró’s paper are the ones of DW UMa and not of GSC 3822-1056. The correct coordinates this latter one for equinox 2000.0 are $\alpha = 10^{\text{h}}33^{\text{m}}58^{\text{s}}$; $\delta = +58^{\circ}52'16''$.

In this paper we present the results of VR_C photometry of GSC 3822-1056 together with the light curve solution and a period analysis.

2. Observations

GSC 3822-1056 was observed together with the novalike eclipsing variable DW UMa with a Wright Instruments 1024 × 1024 CCD camera mounted on the 80 cm “IAC80” telescope at Observatorio del Teide in Tenerife, Spain, operated by Instituto de Astrofísica de Canarias using Johnson-Cousins V and R_C filters (in fact, it was one of the two comparison candidates on the frame, Bíró 2000b). Typical integration times were 20 s for V and 10 s for R_C bands respectively. 2×2 -pixel binning was used to obtain an optimal sampling of the star profiles of $FWHM \sim 3$ pixels, and only a subframe of size 3×7 arcmin, containing DW UMa and the two comparison candidates GSC 3822-1056 (star 1) and GSC 3822-0070 (star 2). In this way the time between frames was shortened to 5 s.

Observing was conducted during 9 nights between 15 February and 8 April 1997. All the observations were carried out under excellent sky conditions, except for the 19/20 February night session which was partially disturbed by clouds. On the first 3 nights two-filter sequential observations were made. During the other observations we used only one filter per eclipse, alternating V and R_C from one cycle to another, to avoid the long delay of 15 s required for filter changes.

Table 1. Log of observations at IAC. Only the data obtained at the below listed nights were used for the light curve solutions.

JD – 2 400 000	Filters, observing mode
50495	sequential V, R_C
50496	sequential V, R_C
50497	sequential V, R_C
50498	alternating from cycle to cycle V, R_C
50499	alternating from cycle to cycle V, R_C
50500	alternating from cycle to cycle V, R_C
50539	alternating from cycle to cycle V, R_C
50540	alternating from cycle to cycle V, R_C
50547	alternating from cycle to cycle V, R_C

(See Table 1 for a short observational log.) Tables 2a,b list the VR_C data obtained as magnitude differences variable minus comparison in the standard system versus Heliocentric Julian Date.

Calibration standards were observed in four colours on most of the nights to allow for the standard transformation.

The latter was performed by solving the following set of equations:

$$\begin{aligned}
 m_B &= B + b_1 + b_2 X_B + b_3 (B - V) + b_4 (B - V) X_B \\
 m_V &= V + v_1 + v_2 X_V + v_3 (V - R_C) + v_4 (V - R_C) X_V \\
 m_{R_C} &= R_C + r_1 + r_2 X_R + r_3 (V - R_C) + r_4 (V - R_C) X_R \\
 m_{I_C} &= I_C + i_1 + i_2 X_I + i_3 (R_C - I_C) + i_4 (R_C - I_C) X_I
 \end{aligned} \quad (1)$$

where the observed magnitudes are on the left, while the right hand sides contain the standard magnitudes (uppercase letters) and the zero point, extinction and the first and second order colour terms, respectively. The fitted coefficients are marked with lowercase letters, other notations are as usual. The precision of the standard photometry was *unfortunately subverted* by an imperfection of the shutter's timing (see Bíró 2000b for details), which set the main contribution to errors in the standard transformation (they are particularly high for the I -band data, see Table 3), and could be ameliorated to some extent only by the exclusion of frames with exposure times less than 2 s. The above equations were solved separately for each night with standard photometry data. Table 3 shows the obtained values for the coefficients along with their estimated uncertainties.

The zero-point coefficients exhibit significant night-to-night variations. They were taken to be constant within each night; for the other sessions they have been calculated from the condition of constant absolute magnitudes of the comparison star. Average values of the first order colour coefficients were used for all the observations. As for the the second order colour coefficients, the fit yielded (for each night) values of zero within their estimated standard errors; therefore they were considered insignificant and were omitted from the solution.

The data reduction was done with IRAF² by standard methods. The frames were bias and flatfield corrected (dark correction was unnecessary since the camera was cooled by

² IRAF is distributed by the National Optical Astronomical Observatories, operated by the Association of the Universities for Research in Astronomy, Inc., under cooperative agreement with the National Science Foundation.

Table 3. Standard transformation coefficients for the nights with existing standard photometry (blank fields correspond to missing observational data).

Parameter	31 Mar.	1 Apr.	7 Apr.	8 Apr.
b_1	4.966(11)	5.040(18)		4.832(16)
b_2	0.230(07)	0.162(15)		0.384(10)
b_3	-0.237(07)	-0.206(06)		-0.226(07)
b_4	0.0(0)	0.0(0)		0.0(0)
v_1	4.011(16)	4.091(16)	4.018(13)	4.052(09)
v_2	0.157(08)	0.088(13)	0.175(08)	0.142(11)
v_3	-0.009(10)	-0.002(09)	-0.036(08)	-0.002(11)
v_4	0.0(0)	0.0(0)	0.0(0)	0.0(0)
r_1	3.022(20)	3.536(06)	3.472(14)	3.443(02)
r_2	0.510(10)	0.042(12)	0.121(10)	0.159(09)
r_3	0.005(23)	0.010(17)	-0.005(12)	-0.015(20)
r_4	0.0(0)	0.0(0)	0.0(0)	0.0(0)
i_1	3.666(15)	4.100(20)	4.065(22)	4.088(28)
i_2	0.393(09)	0.044(16)	0.108(14)	0.183(12)
i_3	-0.009(23)	-0.072(21)	-0.080(20)	-0.200(30)
i_4	0.0(0)	0.0(0)	0.0(0)	0.0(0)

Table 4. Johnson-Cousins $BV(RI)_C$ colour indices of GSC 3822-1056 at different phases.

Colour	$\varphi = 0.9$	$\varphi = 0.3$	$\varphi = 0.5$
$B - V$	0.48	0.55	0.58
$V - R_C$	0.36	0.34	0.34
$R_C - I_C$	0.42	0.41	0.40
$V - I_C$	0.78	0.75	0.74

liquid nitrogen). Cosmic rays have been carefully removed from each frame. Aperture photometry was then performed for the variable and the two comparison candidates, followed by aperture correction to minimize the magnitude errors (Stetson 1990, task “mkapfile” implemented under IRAF). A typical internal error (as estimated by the IRAF photometry tasks) of the relative photometry is 0.01 mag.

Star 2 (GSC 3822-0070) showed sufficient stability to be employed as a comparison. The standard transformation yielded the following magnitudes for this comparison: $B = 13.92 \pm 0.02$ mag, $V = 13.29 \pm 0.05$ mag, $R_C = 12.88 \pm 0.01$ mag, $I_C = 12.40 \pm 0.04$ mag. Using these values the Johnson-Cousins $BV(RI)_C$ standard magnitudes were determined for GSC 3822-1056. The Johnson-Cousins-colours of the system at certain phases are tabulated in Table 4. The long-wavelength colour indices are very stable during a cycle but $B - V$ varies with 0.1 mag. However, the precision of the $B - V$ is about 0.07 mag, the other colour indices are precise to ± 0.05 mag.

Note that the object shows remarkable O’Connell-effect (the heights of the primary and secondary maxima differ from each other, an effect frequently explained by spot-activity) on the unfiltered light curves obtained at Baja Astronomical Observatory (see Fig. 4). Since the other constant stars on these frames showed a sufficient stability (within 0.03 mag), and the levels of magnitude differences were the same from

night to night, we mind that the light-curve variations showed in Fig. 4 are real and not caused by the variable atmosphere. Note that the variation of the maximum light and the occasionally interchange of the depths of the two minima is common features of contact binary systems. However, in this analysis we did not use the unfiltered observations, but they are listed in Table 2c.

3. Period analysis

A total of 45 times of minima have been observed of this system by the Baja observers since the discovery in 1997. These data were continuously published in the IBVS bulletins (Bíró & Borkovits 2000; Borkovits et al. 2001, 2002); nevertheless, for the sake of the completeness we list them in Table 5. Plotting the O–C diagram with the linear ephemeris:

$$\text{MIN}_1 = 2\,450\,495.5189 + 0.309892E, \quad (2)$$

(see Fig. 1) we can conclude that the period of the system is not constant. The shape of the curve may suggest either a parabolic trend, and/or a partly covered sinusoidal variation. This latter could arise as a consequence of the revolution of the binary around the common centre of mass of a possible triple system (see next section). However, even if the light-time effect is real, at present one can only state that its period is longer than a decade. This is why we omitted this possibility in the following analysis.

Supposing that the period change is constant during a revolution of the binary, using the usual least-squares fit one can obtain the following quadratic ephemeris:

$$\text{MIN}_1 = 2\,450\,495.5213(3) + 0.309889(3)E + 5.67(40) \times 10^{-10}E^2. \quad (3)$$

According to this ephemeris the rate of the continuous period change $dP/dt \approx +1.34 \times 10^{-6} \text{ d yr}^{-1} = +11.6 \text{ s/century}$. Note that the highest rates of similar long-term period increases in W UMa stars are $+2.7 \text{ s/century}$ for V839 Oph (Wolf et al. 1996), $+3.1 \text{ s/century}$ for UZ Leo (Hegedüs & Jäger 1992) and $+5.3 \text{ s/century}$ for XY Boo (Molík & Wolf 1998). However, these rates were based on a data set spread in time longer than our data set and therefore these rates are more reliable than our one. However, the fact of the period increase is unquestionable, but its rate should be checked by future minima observations. Furthermore, we note again, that a certain part of the period increase may come from light-time effect.

4. Light curve solution

The shape of the light curve of GSC 3822-1056 is that of a β Lyr-type binary (see Figs. 2 and 3) and it is very similar to one of what we call poor thermal contact (hereafter PTC) stars (e.g. FO Hyd, see Candy & Candy 1997). The period is very short ($P = 0.31 \text{ days}$) which are similar to the most frequent period of the W UMa-type stars. In the case of such a short period one could expect an (over-)contact configuration. Therefore we chose Mode 3 of the 1998 version of the Wilson-Devinney Code (Wilson 1998). The code is based on

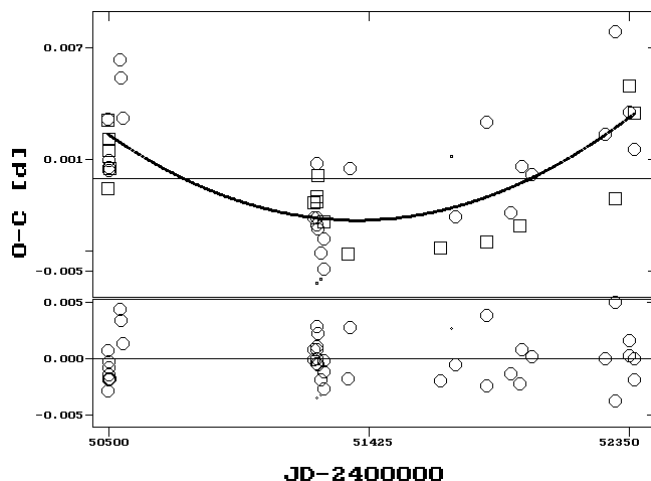


Fig. 1. The linear O–C diagram of GSC 3822-1056 with the quadratic fit (above), and the residuals after the subtraction of this parabola. (Circles denote the primary minima, while rectangles stand for the secondary ones.)

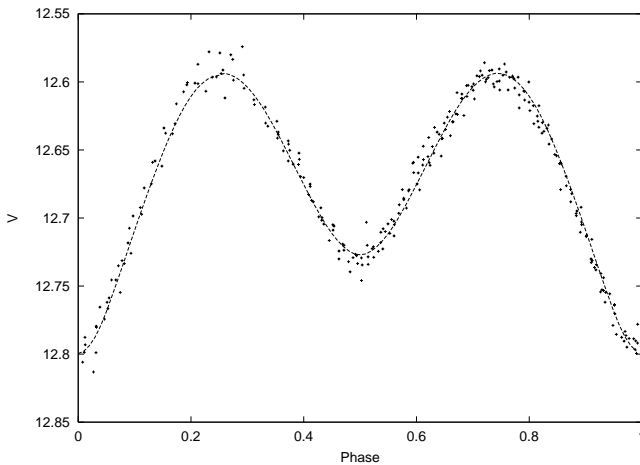
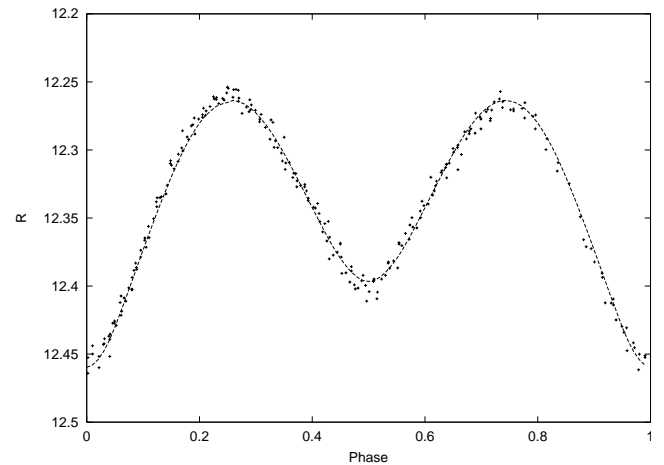
the Wilson-Devinney model which is described in detail by Wilson & Devinney (1971), Wilson et al. (1972), and Wilson (1979). In Mode 3 the limb-darkening coefficients, gravity darkening exponents, albedos and the Ω -values (the latter are in a linearized, dimensionless form of the surface gravity potentials) are the same for both components ($x_1 = x_2, g_1 = g_2, A_1 = A_2, \Omega_1 = \Omega_2$), but the surface temperatures can be adjusted independently from each other. This means that the stars are assumed to be in geometrical, but not in thermal contact. Since we do not know about any spectroscopic measurements on this star, following several authors (e.g. Yang & Liu 2002) we estimated the surface temperature of the primary to be $T_1 = 5500 \text{ K}$ from the colour index of the system. Since the object is located at high galactic latitude ($b = 50^\circ.41$) we assumed that the interstellar reddening is negligible, and we did not correct for it. Bolometric and monochromatic limb-darkening coefficients were taken from van Hamme (1993). Lucy's (1967) values of the gravity darkening exponents ($g_1 = g_2 = 0.32$) and Rucinski's (1969) values of the albedos ($A_1 = A_2 = 0.50$) were applied. The following parameters were adjusted: inclination (i), surface potential of the primary (Ω_1), surface temperature of the secondary (T_2) and the fractional luminosity of the primary (L_1/L_{tot}) (solution B). Black-body radiation was assumed for both components. The mass-ratio is not known due to lack of spectroscopy, therefore we followed the most common way (Branicki & Pigulski 2002) to determine it. The mass-ratio was fixed at several values between 0.1–6.0 and the behaviour of the sum of squares of residuals (SSRs) was used to estimate its value. Since the best fits were not suitable we allowed to adjust the third light (l_3 , we call this solution as solution A) and we also checked the SSRs at the fixed mass-ratios in the same interval. The q –SSRs relations for both cases (solutions A and B) can be seen in Fig. 5.

However, it should be emphasized that third light can modify the original colour indices of the system and that is why perhaps our assumption for the primary's temperature cannot be valid. We investigated this effect in the following way.

Table 5. Times of photoelectric minima of GSC 3822-1056 (HJD–2 400 000). References: (1) Bíró & Borkovits (2000), (2) Borkovits et al. (2001), (3) Borkovits et al. (2002).

Min	Type	Ref.	Min	Type	Ref.	Min	Type	Ref.	Min	Type	Ref.
50495.5221	p	1	51228.4120	p	1	51250.566 ^a	s	1	51925.360	p	2
50495.676	s	1	51228.5678	s	1	51262.345	s	1	51958.3628	s	2
50496.603	s	1	51236.46923	p	1	51262.499	p	1	51967.5078	p	2
50496.7591	p	1	51236.6253	s	1	51263.4271	p	1	52000.3560	p	2
50497.6886	p	1	51237.3985	p	1	51349.423	s	1	52263.4567	p	3
50498.465	s	1	51237.5547	s	1	51356.4002	p	1	52298.480	p	3
50498.6189	p	1	51238.3315	p	1	51675.4300	s	1	52298.626	s	3
50499.7040	s	1	51238.480 ^a	s	1	51715.411 ^a	s	1	52347.4387	p	3
50500.6327	s	1	51242.3566	p	1	51731.3672	p	2	52347.5950	s	3
50539.530	p	1	51242.5144	s	1	51840.6029	s	2	52366.3401	p	3
50540.4587	p	1	51250.4125	p	1	51842.6236	p	2	52366.497	s	3
50547.5841	p	1									

^a These minima times were omitted from the calculations due to the large scatter of the data.

**Fig. 2.** *V*-light curve (points) and its solution (line) of GSC 3822-1056.**Fig. 3.** *R*-light curve (points) and its solution (line) of GSC 3822-1056.

The best solutions were found near $q = 0.85$ and $q = 0.90$. We expanded the adjustable parameters with the mass-ratio starting the iterations from $q = 0.90$. The Method of Multiple Subsets (Wilson & Biermann 1976) was chosen for determining the parameters and investigating the stability of our solution. The first subset consisted of (T_1, q, L_1) and the second one does of (T_2, i, Ω_1, l_3) . The solution converged and we found a mass-ratio of $q = 0.885$. The temperature of the primary was found to be close to the previous one ($T_1 = 5516$ K at reaching the convergence point). The fitting of light curves are shown graphically in Figs. 2 and 3. Solution B was also optimized in a similar way starting from $q = 3.6$ at where the best solution without third light was found. The result can be found in Table 6. As one can see solution A is better than solution B, therefore solution A was accepted for GSC 3822-1056.

The errors in Table 6 are formal errors yielded by the Wilson-Devinney Code. Due to the correlations between the parameters (Maceroni & Rucinski 1997), it should be at least doubled. Despite the fact that there was a correlation between the mass ratio and third light (and therefore there also was a correlation between the inclination and the third light due to

the well-known correlation between the mass ratio and inclination), the presence of third light in the system was not surprising, because the possible existence of a third object is allowed by the interpretation of the O–C diagram (see Sect. 3). Since these correlations might cause some error in the final result, spectroscopic confirmation is required (see below).

The accepted solution A was investigated further because the system shows O’Connell-effect. This was studied with the assumption of a dark spot on the surface of the primary star and of the secondary star, respectively. (When a hot spot on one of the components was assumed, the solution convergence failed.) A dark spot on the secondary yielded a slightly better solution than it is on the primary, but the difference is not significant. (See Table 7.) The spot is located near to the side part of the star which is most obvious at the quadrature. This supports that the deeper minimum is indeed due to global temperature difference between the stars and not due to fortuitously placed spots.

Note that W UMa stars frequently have third companion (Kopal 1978). The occurrence of a third object in the system of GSC 3822-1056 is not unprecedented, but it has relatively high luminosity compared to the close pair. Note that

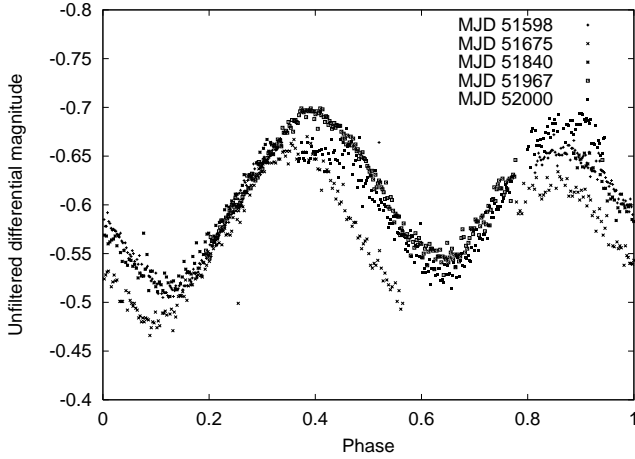


Fig. 4. Unfiltered light curve of GSC 3822-1056 obtained at the Baja Astronomical Observatory showing the O'Connell-effect.

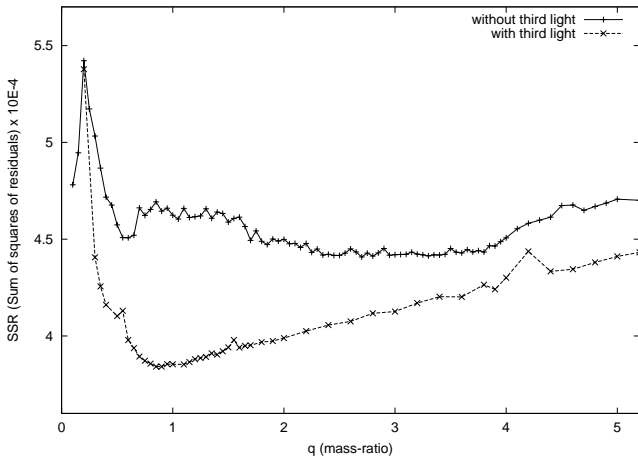


Fig. 5. SSR vs. q diagram with and without third light.

V909 Cygni (although it is an Algol-star object) also has high fractional luminosity third companion (in that case $L_3/L_{\text{total}} \approx 0.22$ in B and V , Lacy et al. 1999). Other Algols, as AC Vel (10–15% third light in y , Johanssen et al. 1997) and DI Peg (22–25% third light in V , Rucinski 1967) also have large third light. The W UMa star 44 Bootis also has a large third light, although its contribution is known a priori (Maceroni et al. 1987). As a consequence, we would like to point out that there are a few cases where the third light can be high enough to produce a large part of the total luminosity and it is likely that we observed a similar feature in GSC 3822-1056.

Note that the light-curve of VZ Piscium which system is similar to GSC 3822-1056 (see the parameters derived by Hrivnak & Milone 1989) can alternatively be modeled (Maceroni et al. 1990). Therefore we tried to solve the light curve of GSC 3822-1056 in Mode 5 of the Wilson-Devinney Code. This mode means a semi-detached configuration. Our free parameters were q (mass-ratio), i , T_2 , Ω_2 , L_1/L_{tot} . This solution yielded a sum of squares of residuals of 4.16×10^{-3} . This value is higher than that of solution A and therefore we can omit the possibility that GSC 3822-1056 is a semi-detached binary. When we adjusted the third light in Mode 5, a “semi-over-contact” configuration was found: the primary overflowed

Table 6. Photometric solutions of GSC 3822-1056.

Parameter	$l_3 \neq 0$ solution A		$l_3 = 0$ solution B	
	Value	Error	Value	Error
$L_1/(L_1 + L_2 + L_3)$				
V:	0.3270	0.0327	0.5220	0.0168
R:	0.3132	0.0315	0.4538	0.0139
$L_3/(L_1 + L_2 + L_3)$				
V:	0.5757	0.0546	0	
R:	0.5683	0.0526	0	
$x_1 = x_2$				
bolometric:	0.477		0.477	
V:	0.644		0.644	
R:	0.556		0.556	
$q = M_2/M_1$	0.886	0.015	3.682	0.025
i	62.84	1.35	49.43	0.33
$A_1 = A_2$	0.50		0.50	
$g_1 = g_2$	0.32		0.32	
$\Omega_1 = \Omega_2$	3.2811	0.0157	7.4191	0.0248
T_1	5516 K	120 K	5500 K	
T_2	4471 K	240 K	4350 K	180 K
r_1 (pole)	0.4064	0.0033	0.2600	0.0022
r_1 (side)	0.4368	0.0046	0.2715	0.0027
r_1 (back)	0.4954	0.0092	0.3094	0.0050
r_2 (pole)	0.3866	0.0035	0.4698	0.0015
r_2 (side)	0.4142	0.0049	0.5080	0.0021
r_2 (back)	0.4777	0.0107	0.5344	0.0027
$\Sigma w(l_{\text{obs}} - l_{\text{comp}})^2$	3.87×10^{-3}		4.80×10^{-3}	

its Roche-lobe, the secondary filled exactly its own one. Since this is out of the prescribed limits of the solution (see the description of Mode 5 in Wilson 1998), and this yielded a weaker fit, this solution was also omitted.

If the high contribution of the third light is real, its source can belong physically to the system. However, in this case the following observational consequences should exist:

(i) The spectrum of GSC 3822-1056 is a composite spectrum of three stars because of the almost equal luminosities of the stars. Although the object is moderately faint ($V_{\text{max}} \sim 12^m6$), it would be interesting to check its spectrum. Note that this can also be observed, even if the third object is not a physical companion. However, this would prove our solution.

(ii) Although the orbital period of the third object is presently unknown, the orbital revolution around the common mass centre some light-time effect may be observed in the future. The minima of this eclipsing variable has been observed since 1997 and this time-coverage is not long enough to say anything about the presence of light-time effect. So, the O–C diagram would show the corresponding periodic term if the third body’s theorem has reality and if the inclination of the third body’s orbit is favourable. Its inclination also influences the rate of the following effect:

(iii) The gamma velocity of the close inner pair should show some variations with time due to the motion on the wide orbit. The variation may be observable within some years.

Table 7. Spot parameters for a dark spot on the primary (first row), or on the secondary (last row).

Star	Lat.	Long.	Radius	Temp. factor	Σwr^2
Pri.	-48(15)°	86(9)°	17(5)°	0.10(2)	3.681×10^{-3}
Sec.	-30(14)°	261(7)°	17(6)°	0.30(5)	3.671×10^{-3}

Table 8. Estimated absolute dimensions of GSC 3822-1056.

Star	Mass (M_{\odot})	Radii (R_{\odot})	Bol. lum. (L_{\odot})
Primary	0.75	0.95	0.75
Secondary	0.66	0.90	0.29

5. Absolute dimensions

The absolute dimensions of GSC 3822-1056 can roughly be estimated via the Rucinski-Duerbeck's PLC-calibration (Rucinski & Duerbeck 1997). It has the following form:

$$M_V = -4.42 \log P + 3.08(B - V) + 0.10. \quad (4)$$

Close to the maximum the $B - V \approx 0.55$ mag (see Table 1) and the period is 0.30988 days. Hence $M_V = 4.04^{+0.83}_{-0.54}$. Most of the errors come from the uncertainties of the PLC-calibration. We assumed that the interstellar reddening is negligible in the direction of GSC 3822-1056, so the distance of the system is 513^{+145}_{-163} parsec accepting $V = 12.59$ (Bíró 2000a). From the absolute magnitude the visual and bolometric luminosities can be computed. (We used Flower's 1996 tables to determine the bolometric correction from the temperatures.) Then one can apply $L = \text{constant} \times R^2 T^4$ and $R_{1,2} = Ar_{1,2}$ from which we can estimate the semi-major axis. Applying Kepler's third law and the photometrically determined mass-ratio the individual masses of the components can be calculated. The results are presented in Table 8. The semi-major axis of the system is $2.17 R_{\odot}$.

The colour index of the tertiary component can be estimated on the same way as described in Borkovits et al. (2002). The referred equation is

$$(V - R)_3 = -2.5 \left[\log \left(\frac{L_{3,V}}{L_{3,R}} \right) - \log \left(\frac{L_{1,V}}{L_{1,R}} \right) \right] + (V - R)_1 \quad (5)$$

where $(V - R)_i$ is referring to the i th component's colour index, $L_3 \approx 4\pi l_3$ where l_3 is the third light obtained from the light curve solution, and the luminosities of the components are given in arbitrary units as used by Wilson-Devinney Code. We found that the difference between the $V - R$ colour index of the primary and the tertiary is only 0^m03. Colour indices of each component are listed in Table 9. Note that the colour index of the tertiary was estimated applying Eq. (5) while primary's and secondary's colour index was guessed from their temperatures.

It is interesting to examine the position of the components on the HRD. Using the empirical HRD constructed from HIPPARCOS data by de Bruijne et al. (2001), one can see that the primary star is on the main sequence, however, the secondary is slightly above the main sequence.

Table 9. $V - R_C$ colour indices of the components estimated from the light curve solution.

Component	$V - R_C$
Primary	0.432
Secondary	0.733
Tertiary	0.465

6. Summary and discussion

We present the first CCD two-colour VR_C photometry of GSC 3822-1056. A period analysis and a light-curve solution were carried out. The period study revealed a rapid period increase, but the effects of a possible third body and the continuous period variation presently are inseparable. However, the period increase is obvious. The light-curve solution yielded an unusual A-type system³. These unusual properties are discussed below.

Although GSC 3822-1056 is in deep contact (the fill-out factor $f = (\Omega_{\text{inner}} - \Omega) / (\Omega_{\text{inner}} - \Omega_{\text{outer}}) = 0.57$), its components seem to be far from thermal contact ($\Delta T = T_1 - T_2 = 1045$ K). In the present physical state of the system, the behaviour of the orbital period is in good correspondence with the magnetically driven angular momentum loss (AML) hypothesis (Van't Veer 1979; Van't Veer & Maceroni 1989). This theory predicts that in the contact stage the magnetic torque can cause contact binaries to evolve to extremely low mass ratios which suggests a mass transfer from the secondary to the more massive primary and consequently we have to observe period increasing. The AML theory predicts that near $q = 1$ the variation of the period is very fast, and these are in good agreement with our observational results.

The AML theory requires intensive magnetic activity in the system. Our five-year long photometric monitoring of this system gives some indirect evidence for the presence of magnetic activity. As seen in Fig. 4 the shape of the light curves, the height of the minima and the maxima changed month by month. These distorted light curves and the strong O'Connell effect might be the consequences of stellar activity, e.g. starspots. The large scatter of the O - C residuals can also be explained by the magnetically distorted light curves. Note that according to Kalimeris et al. 2002 an average-sized spot on the primary component can cause a shift in the observed time of mid-eclipse in the same order which is the scatter of our curve.

According to the theoretical computation of Sarna & Fedorova (1989), a high mass-ratio ($q > 0.25$) A-type system has a temperature difference of $\Delta T = 2000 - 3000$ K between the components after reaching the contact stage. According to them the temperature excess of the secondary is caused by the heating mechanism of the accreted matter. Although we can only speculate about the evolutionary state of the system, the whole picture suggest that GSC 3822-1056 may be a recently formed contact binary. However, since our light curve solution should be supported by future spectroscopic facts (see Sect. 4),

³ Classical W UMa-type stars are divided into two classes: A-type (larger star slightly hotter) and W-type (smaller star slightly hotter).

to relate it to the early state of the AML, further spectroscopic and photometric observations are needed to refine the physical parameters of the system.

Acknowledgements. This research has made use of NASA's Astrophysics Data System Abstract and Article Service. We thank Drs L. Patkós and L. Szabados for their kind help and advice during the preparation of the manuscript. This work was supported by the Hungarian OTKA Grant T034551 and T030743. I. B. Bíró wishes to thank Carlos Lázaro for being his supervisor during his grant period at IAC. The support of Szécsenyi István Scholarship Foundation, Hungary is also acknowledged.

References

- Bíró, I. B. 2000a, IBVS, No. 4929
 Bíró, I. B. 2000b, A&A, 364, 573
 Bíró, I. B., & Borkovits, T. 2000, IBVS, No. 4967
 Borkovits, T., Bíró, I. B., & Kovács, T. 2001, IBVS, No. 5206
 Borkovits, T., Bíró, I. B., Hegedüs, T., et al. 2002, IBVS, No. 5313
 Borkovits, T., Csizmadia, Sz., Hegedüs, T., et al. 2002, A&A, 392, 895
 Branicki, A., & Pigulski, A. 2002, IBVS, No. 5280
 de Bruijne, J. H. J., Hoogerwerf, R., & de Zeeuw, P. T. 2001, A&A, 367, 111
 Candy, M. P., & Candy, B. N. 1997, MNRAS, 286, 229
 Flower, P. J. 1996, ApJ, 469, 355
 Hegedüs, T., & Jäger, Z. 1992, PASP, 104, 733
 Hrivnak, B. J., & Milone, E. F. 1989, AJ, 97, 532
 Johanssen, K. T., Helt, B. E., & Clausen, J. V. 1997, IBVS, No. 4520
 Kalimeris, A., Rovithis-Livaniou, H., & Rovithis, P. 2002, A&A, 387, 969
 Kopal, Z. 1978, Dynamics of Close Binaries (University of Dordrecht)
 Lacy, C. H., Zakirov, M., Arzumanyants, G. C., et al. 1999, IBVS, No. 4782
 Lucy, L. B. 1967, Z. Astrophys., 65, 89
 Maceroni, C., Milano, L., Russo, G., & Sollazzo, C. 1987, A&AS, 45, 187
 Maceroni, C., van Hamme, W., & van't Veer, F. 1990, A&A, 234, 177
 Maceroni, C., & Rucinski, S. M. 1997, PASP, 109, 782
 Martin, B. E. 2000, IBVS, No. 4880
 Molík, P., & Wolf, M. 1998, IBVS, No. 4640
 Rucinski, S. M. 1967, AcA, 17, 271
 Rucinski, S. M. 1969, A&A, 19, 245
 Rucinski, S. M., & Duerbeck, H. W. 1997, PASP, 109, 1340
 Sarna, M. J., & Fedorova, A. V. 1989, A&A, 208, 111
 Stetson P. 1990, PASP, 102, 932
 van Hamme, W. 1993, AJ, 106, 2096
 Van't Veer, F. 1979, A&A, 80, 287
 Van't Veer, F., & Maceroni, C. 1989, A&A, 220, 128
 Wilson, R. E. 1979, ApJ, 234, 1054
 Wilson, R. E. 1998, Computing Observable Binary Stars (University of Florida)
 Wilson, R. E., & Biermann, P. 1976, A&A, 48, 349
 Wilson, R. E., & Devinney, J. 1971, ApJ, 166, 605
 Wilson, R. E., de Luccia, M., Johnston, K., & Mango, S. A. 1972, ApJ, 177, 191
 Wolf, M., Sarounová, L., & Molík, P. 1996, IBVS, No. 4304
 Yang, Y., & Liu, Q. 2002, AJ, 123, 443